This article was downloaded by: [Amor Ben Moussa]
On: 04 January 2012, At: 02:26
Publisher: Taylor & Francis
Informa Ltd Registered in England and Wales Registered Number: 1072954 Registered office: Mortimer House, 37-41 Mortimer Street, London W1T 3JH, UK



Arid Land Research and Management
Publication details, including instructions for authors and subscription information:
http://www.tandfonline.com/loi/uasr20

Hydrogeochemical Analysis of Groundwater Pollution in an Irrigated Land in Cap Bon Peninsula, North-Eastern Tunisia

Amor Ben Moussa [a], Kamel Zouari [a], Vincent Valles [b] & Fayçal Jlassi [c]

[a] National Engineering School of Sfax, Sfax, Tunisia
[b] Hydrogeology Laboratory of Avignon, Avignon, France
[c] Agricultural Development of Nabeul, Nabeul, Tunisia

Available online: 03 Jan 2012

To cite this article: Amor Ben Moussa, Kamel Zouari, Vincent Valles & Fayçal Jlassi (2012): Hydrogeochemical Analysis of Groundwater Pollution in an Irrigated Land in Cap Bon Peninsula, North-Eastern Tunisia, Arid Land Research and Management, 26:1, 1-14

To link to this article: http://dx.doi.org/10.1080/15324982.2011.631688

PLEASE SCROLL DOWN FOR ARTICLE

Full terms and conditions of use: http://www.tandfonline.com/page/terms-and-conditions

This article may be used for research, teaching, and private study purposes. Any substantial or systematic reproduction, redistribution, reselling, loan, sub-licensing, systematic supply, or distribution in any form to anyone is expressly forbidden.

The publisher does not give any warranty express or implied or make any representation that the contents will be complete or accurate or up to date. The accuracy of any instructions, formulae, and drug doses should be independently verified with primary sources. The publisher shall not be liable for any loss, actions, claims, proceedings, demand, or costs or damages whatsoever or howsoever caused arising directly or indirectly in connection with or arising out of the use of this material.

Arid Land Research and Management, 26:1–14, 2012
Copyright © Taylor & Francis Group, LLC
ISSN: 1532-4982 print/1532-4990 online
DOI: 10.1080/15324982.2011.631688

Taylor & Francis
Taylor & Francis Group

Hydrogeochemical Analysis of Groundwater Pollution in an Irrigated Land in Cap Bon Peninsula, North-Eastern Tunisia

Amor Ben Moussa[1], Kamel Zouari[1], Vincent Valles[2], and Fayçal Jlassi[3]

[1]National Engineering School of Sfax, Sfax, Tunisia
[2]Hydrogeology Laboratory of Avignon, Avignon, France
[3]Agricultural Development of Nabeul, Nabeul, Tunisia

Downloaded by [Amor Ben Moussa] at 02:26 04 January 2012

Situated in semi-arid regions of northern Africa, the Nabeul-Hammamet basin, North-eastern Tunisia, is a typical alluvial plain, where rural population relies exclusively on groundwater as a water-supply source. Major ions hydrochemistry was used in conjunction with hydrogeological data to understand the aquifer hydrodynamic functioning and to identify natural and anthropogenic salinisation processes. An attempt has been made to recognize these processes using Principal Components Analysis (PCA) and bivariate diagrams of major element data. The groundwater composition is extensively modified by the water–rock reaction in the subsurface, that is, dissolution of halite, gypsum, and/or anhydrite; and ion-exchange with phyllosilicates. Nevertheless, overall groundwater samples are characterized by relatively high nitrate contents suggesting that the return flow of irrigation waters is a significant source of the groundwater contamination.

Keywords dissolution, groundwater, natural and anthropogenic process, nitrate, return flow, salinization

Throughout history, groundwater resources are of major concern and vital to the economic development of all North African countries. In recent years, urban and intense agricultural development has created high demand on groundwater resources in the Nabeul-Hammamet coastal basin, which hosts a large number of wells tapping the Plio-Quaternary unconfined aquifer. Some of these wells are used for drinking water, and about 80% of the water is used for irrigation. The high withdrawal rates, which are required to confront the increasing demands of the agricultural practices, had led to depletion of the groundwater resources and degradation of their quality. Indeed, the agricultural production that is based essentially on flood irrigation and potential application of fertilizer to improve the soils has permanently increased the risk of water scarcity and groundwater quality deterioration. As examples of water-supply related problems, the generalized water-level decline and the potential

Received 19 July 2010; accepted 8 June 2011.
Address correspondence to Amor Ben Moussa, National Engineering School of Sfax, B. P. "W", Sfax 3038, Tunisie. E-mail: amor_geologie@yahoo.fr

contamination of groundwater by evaporitic salts and nitrate leached downward are most prominent. Being a fundamental resource for the region, the studied unconfined aquifer is of major economic importance, which needs to be carefully assessed and managed.

For this study, hydrogeological and hydrochemical data from groundwater of the studied shallow aquifer will be integrated and used to determine the main factors and mechanisms controlling the chemical composition of groundwater in the area.

Study Area

The study area is part of the Cap Bon peninsula and lies between the latitudes 36°22′–36°32′ N and the longitudes 10°32′–10°42′ E. The basin encompasses an area of about 450 Km^2 with an altitude ranging from about sea level to 500 m above sea level. It is limited in the west by the Bouficha plain, in the north by the Grombalia basin, in the east by the oriental coastal plain and in the south by the Gulf of Hammamet (Figure 1). Climatic data compiled from the Nabeul station indicate that the study area is distinguished by a warm Mediterranean climate. The mean annual rainfall, evapotranspiration, and temperature are 450 mm, 1,350 mm, and 25°C, respectively. The investigated basin is drained by several ephemeral Wadis collecting rainwater from the foot of hills in the direction of the Mediterranean Sea. It is densely populated, highly urbanized, and is characterized by touristic, commercial, residential, and agricultural land uses.

Downloaded by [Amor Ben Moussa] at 02:26 04 January 2012

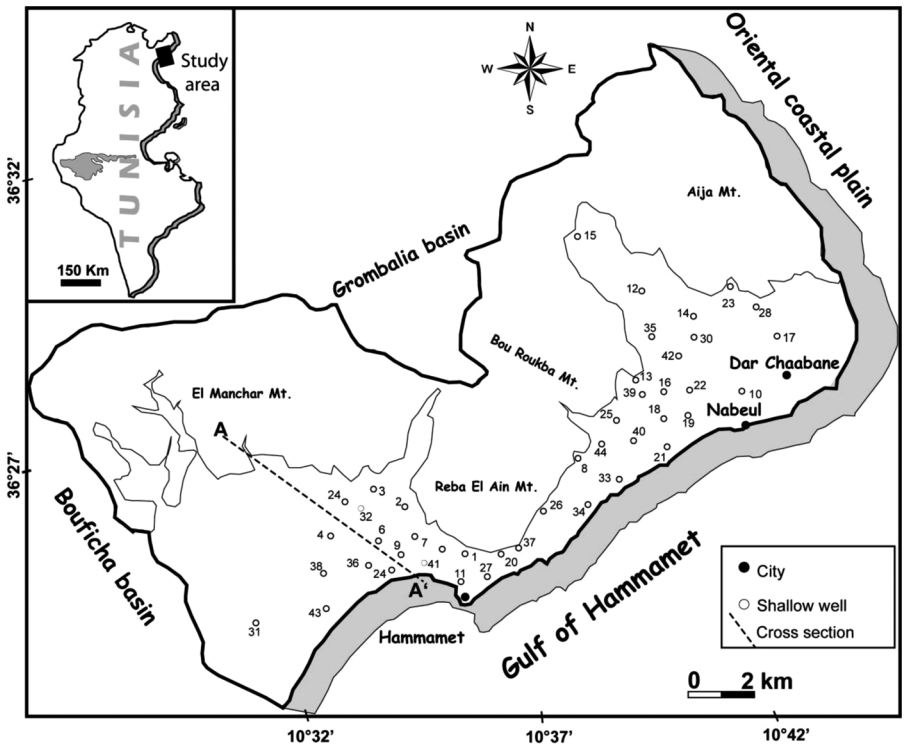

Figure 1. Location and sampling map.

Downloaded by [Amor Ben Moussa] at 02:26 04 January 2012

Geology and Hydrogeology

Geologically, the sedimentary Formations, which out crop in the study area, are represented by the Eocene, Oligocene, Miocene, Pliocene and the Quaternary series (Figure 2). The Eocene deposits consist mainly of the limestone of Bou Dabbous Formation, which is covered by the marl of the Souar Formation (Ben Salem 1995). The Eocene units are overlaid unconformably by the Oligocene deposits, which are made up of sandstone of the Fortuna Formation (Burollet 1956; Blondel 1991). This Formation is covered by the Burdigalian clayey sands, sands and sandstone of the Massiouta Formation, which is overlain by the Langhian limestone and gypseous marl of the Ain Ghrab and Mahmoud Formations, respectively. Above, lay the fine to medium grained sands deposits of the Beglia Serravalian Formation and the clay and marly clay series of the Souaf Tortonian Formation (Ben Salem, 1995). On the Souaf deposits, repose the sandy units of the Somâa and Beni Khiar Tortonian Formations, which are overlain by the sandy sandstone of the Oued el Bir Messinean Formation (Schoeller, 1939). The Plio-Quaternary Formations, which overlay the Miocene series, are represented by the Lower Tabianian clay of Potters, the Upper Tabianian sands of Nabeul, the Lower Plaisancian clay of Sidi Barka, the sandstones of the Upper Plaisancian and the sands of the Quaternary (Colleuil, 1976).

Tectonically, the basin was exposed, since the Pliocene, to a complex tectonic event (Mzali & Zouari, 2006). In fact, this tectonic phase has contributed to the creation of NE–SW folds structures in relation with NE–SW and E-W to N120 reverse faults (Mzali & Zouari, 2006; Mzali et al., 2007).

Hydrogeologically, the shallow aquifer, which is unconfined overall the basin, is lodged in the Plio-Quaternary detrital deposits (Figure 2). It consists mainly of sandstone, sand, clay, and evaporates. This unconfined aquifer, which is tapped by numerous personal and public owned wells, represents the principal source of water supply probably due to its significant permeability and transmissivity. The bedrock

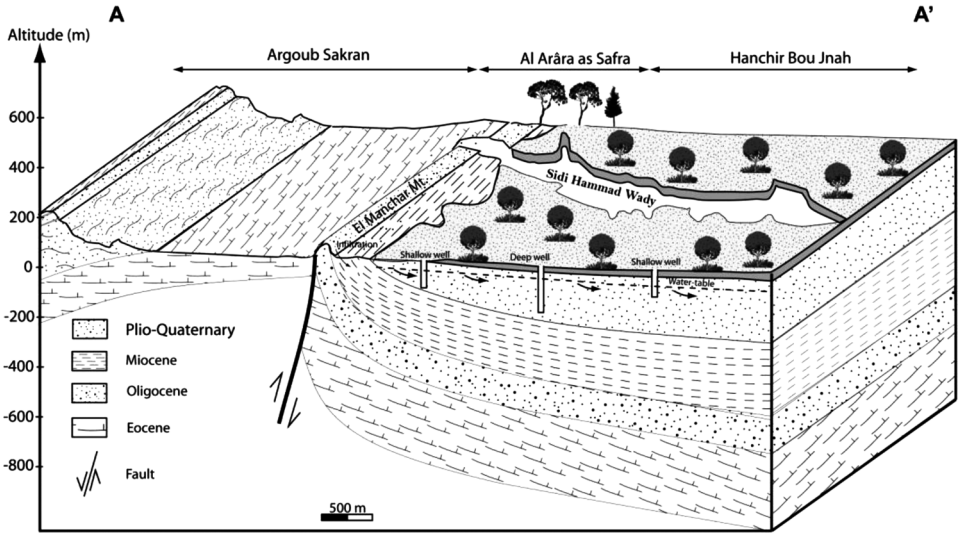

Figure 2. Hydrogeologic cross section in the southern Cap Bon unconfined aquifer.

aquifer is made up of Miocene clayey deposits, which separate it from the Oligocene underlying confined aquifer. The general direction of groundwater flow is toward the Gulf of Hammamet from the foot of El Manchar, Reba el Ain, Bou Rokba, and Aija mountains.

Materials and Methods

A total of 44 wells were sampled, during March 2008, for hydrochemical analyses (Figure 1). Physicochemical parameters were determined at each sampling point. Chemical analyses were undertaken in the "Laboratoire de Radio-Analyses et Environnement," Sfax, Tunisia. Major cation concentrations were performed on a Waters Ion chromatograph using IC-PakTM CM/D columns. Major anion concentrations were measured using a Metrohm ion chromatograph equipped with CI SUPER-SEP columns. The analysis of bicarbonate was undertaken by titration to the methyl orange endpoint.

Downloaded by [Amor Ben Moussa] at 02:26 04 January 2012

Results and Discussion

The partial pressure of carbon dioxide (pCO_2) was estimated by using WATEQ4 F program (Ball & Nordstrom, 1991). The pCO_2 values, physical parameters, salinity, and major ions concentration are given in Table 1. The values of log (pCO_2) vary between -4.3 and -1.9 with an average of -2.5. The highest values characterize wells located downstream suggesting an increase along a groundwater flow path. This may reflect the relatively longer residence times, which provide insight into the more extensive water-rock interaction and the microbial mediated reactions (Rightmire, 1978; Adams et al., 2001).The lowest values are registered upstream, at the foot of bordering mountains, highlighting the significance of the fresh waters infiltration. The T°C and pH range from 14.6 to 22.5°C and from 7.3 to 9.1, respectively. The Electrical Conductivity (EC) and the salinity values vary largely from 0.7 to $10\,mS \cdot cm^{-1}$ and from 438 to 7234 mg/l, respectively. The salinity contents increase in the direction of groundwater flow. The highest values are measured upstream the basin, indicating both the lack of rainwater infiltration and the relatively longer residence time that favors the dissolution of minerals.

Major Ions Geochemistry

The Chadha diagram was established to precisely recognize the different groundwater facies (Chadha, 1999). The data plotted in this diagram show that groundwater samples fall in the fields 7 and 6 (Figure 3). These arrangements show that strong acid anions (Cl^- and SO_4^{2-}) surpass weak acid anions (HCO_3^- and CO_3^{2-}). The difference between groundwater samples lying in field 6 (Ca-SO_4-Cl water type) and field 7 (Na–Cl water type) is that calcium and magnesium concentrations exceed sodium and potassium contents.

Origin of Mineralization

The examination of correlation matrix can provide valuable insight into the main hydrochemical processes. It can also specify the contribution of the hydrochemical variables to the groundwater mineralization (Helena et al., 2000). The correlation

Downloaded by [Amor Ben Moussa] at 02:26 04 January 2012

Table 1. Physico-chemical data of groundwater samples

Samples no	Latitude	Longitude	Altitude (m)	Cl	NO_3	SO_4	HCO_3	Na	Mg	Ca	Saturation Indexes		Depth (m)	log pCO_2	Salinity (mg/l)	pH	Cond (µS/cm)	T (°C)
							mg/l				halite	gypsum						
1	36° 23′ 09″	10°36′ 29″	20	442.2	182.9	165.3	244.0	269.9	55.1	164.3	−5.5	−1.3	–	−2.4	1524	7.7	2,5	20.2
2	36° 25′ 20″	10° 35′ 40″	15	173.7	125.7	200.7	280.6	114.8	61.3	112.9	−6.3	−1.3	29.2	−2.3	1070	7.56	1,8	19.8
3	36° 25′ 46″	10° 35′ 40″	22	229.2	65.9	147.2	256.2	138.0	38.7	121.7	−6.1	−1.3	35.1	−2.4	997	7.6	1,7	20.1
4	36° 24′ 57″	10° 33′ 50″	12	1689.5	29.4	2142.3	622.2	950.8	325.1	485.2	−4.5	−0.2	15.3	−4.1	6244	7.8	8,2	18.5
5	36° 23′ 19″	10° 34′ 04″	7	440.0	127.5	340.4	378.2	287.7	92.4	189.6	−5.5	−1.0	15	−1.9	1856	7.3	2,7	19.2
6	36° 24′ 44″	10° 34′ 54″	13	586.0	203.9	499.0	183.0	347.3	82.6	219.7	−5.3	−0.8	18.5	−3.0	2121	8.12	3,4	20.7
7	36° 24′ 25″	10° 36′ 29″	16	604.7	345.2	207.1	268.4	300.7	101.1	180.8	−5.4	−1.2	25	−2.0	2008	7.32	3,2	19.8
8	36° 25′ 42″	10° 40′ 06″	12	645.8	135.7	788.1	280.6	413.7	132.9	297.3	−5.2	−0.5	25.6	−2.7	2694	8.03	3,8	18.8
9	36° 23′ 13″	10° 34′ 20″	13	343.7	83.1	326.9	183.0	184.1	57.0	179.9	−5.8	−0.9	26.6	−2.8	1358	7.9	2,2	19.4
10	36° 25′ 24″	10° 41′ 11″	15	470.5	189.8	505.5	390.4	344.6	109.2	171.7	−5.4	0.9	4.75	−2.4	2182	7.7	3,6	21.2
11	36° 22′ 18″	10° 36′ 09″	9	212.5	11.0	212.5	427.0	178.1	48.4	120.6	−6.0	−1.2	6.45	−2.5	1210	7.8	1,8	20
12	36° 29′ 06″	10° 41′ 57″	64	265.1	7.8	94.3	244.0	152.2	43.3	89.4	−6.0	−1.6	16.5	−2.8	896	7.9	1,3	19.6
13	36° 26′ 50″	10° 42′ 14″	25	838.9	55.3	1282.6	323.3	561.0	148.8	380.9	−5.0	−0.3	13.2	−2.7	3591	7.8	5,1	19.7
14	36° 29′ 22″	10° 42′ 26″	12	675.7	165.3	1191.4	414.8	527.2	206.0	357.9	−5.1	−0.4	18.94	−2.5	3538	8	4,8	16.2
15	36° 31′ 13″	10° 39′ 14″	15	68.8	0.0	58.0	195.2	50.4	25.2	40.1	−7.0	−2.1	4.1	−4.3	438	9.16	0,7	20
16	36° 27′ 11″	10° 42′ 47″	23	867.5	265.4	923.8	475.8	622.3	149.0	345.0	−4.9	−0.5	11	−1.9	3649	7.4	4,8	20
17	36° 30′ 11″	10° 42′ 04″	10	785.0	178.6	830.0	305.0	508.6	127.9	306.3	−5.1	−0.5	9.1	−2.5	3042	7.8	4,4	20.8
18	36° 26′ 14″	10° 41′ 57″	9	1334.9	425.1	1961.5	305.0	955.3	236.5	605.1	−4.6	−0.1	9.8	−2.1	5823	7.6	6,9	19.4
19	36° 24′ 25″	10° 36′ 23″	16	1711.0	179.9	2048.7	378.2	1092.6	274.9	587.9	−4.5	−0.1	10	−2.2	6273	7.5	9,3	19.7
20	36° 22′ 11″	10° 36′ 29″	10	154.1	80.4	140.2	207.4	145.3	30.9	79.7	−6.2	−1.5	40	−2.7	838	7.9	1,3	21.3
21	36° 25′ 24″	10° 41′ 05″	10	962.6	0.0	1313.0	402.6	1020.2	123.9	162.1	−4.7	−1.5	3.8	−2.4	3985	7.7	5,7	19
22	36° 28′ 10″	10° 43′ 14″	24	948.6	192.7	977.3	280.6	767.5	97.1	154.9	−4.8	−1.7	14.5	−2.8	3419	7.5	4,9	22.5
23	36° 30′ 24″	10° 42′ 26″	20	255.6	92.6	118.8	237.9	196.6	38.5	66.6	−5.9	−0.6	16.4	−2.8	1007	8	1,6	19.8
24	36° 25′ 50″	10° 34′ 43″	18	227.3	15.5	227.4	317.2	198.3	49.4	68.4	−5.9	−1.7	10.75	−2.9	1104	8.01	1,9	17.4
25	36° 26′ 50″	10° 42′ 14″	15	110.3	40.0	237.4	329.4	157.4	32.0	77.1	−6.4	−0.9	9.7	−2.6	984	7.8	1,3	19.7
26	36° 24′ 04″	10° 36′ 29″	25	140.2	81.4	137.4	305.0	176.5	40.6	61.1	−6.2	−2.0	24.3	−2.7	942	8	1,4	18.9

(*Continued*)

Downloaded by [Amor Ben Moussa] at 02:26 04 January 2012

Table 1. Continued

Samples no	Latitude	Longitude	Altitude (m)	Cl	NO_3	SO_4	HCO_3	Na	Mg	Ca	Saturation Indexes		Depth (m)	log pCO_2	Salinity (mg/l)	pH	Cond (µS/cm)	T (°C)
							mg/l				halite	gypsum						
27	36° 22′ 11″	10° 36′ 06″	12	555.1	71.1	308.5	329.4	401.0	83.2	93.0	−5.3	−1.3	12.1	−2.2	1841	7.4	3,2	21.1
28	36° 29′ 22″	10° 41′ 21′	25	2297.3	330.4	1221.0	286.7	1290.0	151.6	600.2	−4.2	−1.5	18.4	−2.2	6177	7.5	9,6	19
29	36° 24′ 18″	10° 38′ 39″	25	1132.9	138.6	938.6	963.8	905.9	187.5	371.4	−4.7	0.1	16	−2.6	4639	8.24	6	19.8
30	36° 28′ 10″	10° 43′ 14″	24	618.5	280.5	645.3	366.0	593.3	131.8	180.6	−5.1	−0.7	12.7	−2.0	2816	7.6	3,9	20.5
31	36° 23′ 25″	10° 30′ 15″	10	2535.2	28.5	1325.0	512.4	1507.7	216.3	492.2	−4.1	−0.7	18	−2.3	6617	7.6	10	19.8
32	36° 25′ 46″	10° 34′ 55″	20	759.9	93.3	434.2	268.4	456.9	106.5	173.0	−5.1	−1.7	23	−2.3	2292	7.5	3,6	19.7
33	36° 24′ 05″	10° 39′ 04″	10	861.7	0.0	1156.5	536.8	725.3	189.6	199.5	−4.9	−1.4	10.6	−2.3	3669	7.64	5,3	14.6
34	36° 24′ 20″	10° 38′ 06″	10	447.5	17.1	474.4	292.8	348.0	70.3	152.4	−5.4	−1.3	7.55	−2.4	1802	7.6	2,8	20.7
35	36° 29′ 05″	10° 41′ 56″	30	473.5	132.7	551.9	305.0	370.6	84.0	176.1	−5.4	−1.6	14.4	−2.4	2094	7.6	3,2	19.8
36	36° 24′ 15″	10° 34′ 40″	13	1018.2	156.8	987.1	317.2	635.4	143.0	318.2	−4.9	−1.3	8	−2.3	3576	7.41	5,1	20.8
37	36° 23′ 13″	10°35′ 04″	12	1362.0	116.9	723.4	183.0	726.1	125.2	348.6	−4.7	−0.3	24	−3.0	3585	8.1	5,7	19.7
38	36° 24′ 14″	10° 33′ 34″	13	563.6	15.3	116.9	732.0	502.0	59.4	103.6	−5.2	−0.5	15	−2.8	2093	8.3	3,7	17.8
39	36° 27′ 11″	10° 42′ 47″	23	1925.7	0.0	2579.8	329.4	1484.7	284.3	630.0	−4.3	−0.8	16.6	−2.0	7234	7.4	8,9	20.7
40	36° 28′ 04″	10° 42′ 42″	15	1076.1	211.9	1005.1	390.4	786.0	137.1	299.4	−4.8	−0.3	34.2	−2.6	3906	7.9	4,4	21
41	36° 23′ 35″	10° 34′ 24″	10	536.5	105.3	350.2	317.2	428.4	64.1	194.6	−5.3	−0.9	6	−2.3	1996	7.71	3,4	18.5
42	36° 29′ 05″	10° 41′ 56″	27	584.1	186.9	755.8	329.4	519.6	82.4	231.4	−5.2	−0.6	16.4	−2.2	2690	7.5	3,8	20.5
43	36° 24′ 14″	10° 33′ 34″	10	2275.0	0.0	1182.6	451.4	1532.0	199.1	296.3	−4.2	−0.9	7	−2.9	5936	8.18	7,9	18
44	36° 25′ 56″	10° 40′ 28″	24	911.2	244.5	886.8	329.4	734.5	152.7	181.3	−4.8	−0.8	34	−3.1	3440	8.4	4,9	18.4

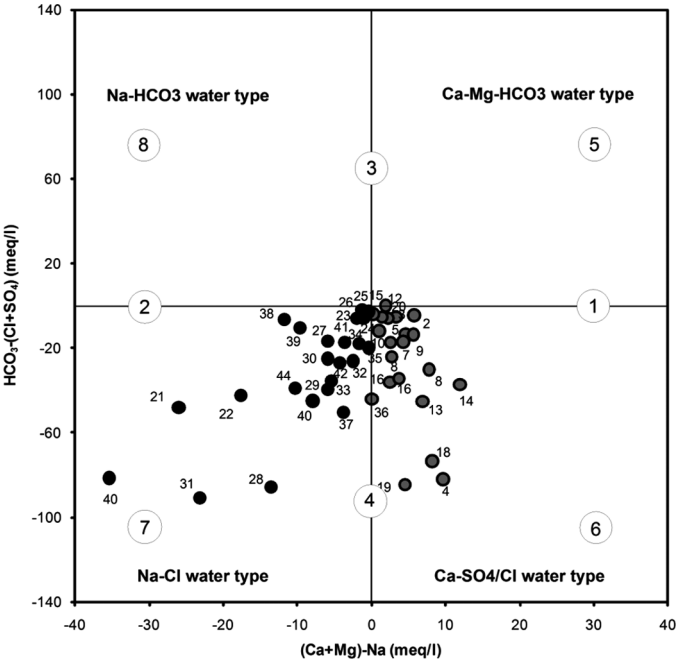

Figure 3. Chadha diagram of the unconfined aquifer groundwaters.

matrix of seven variables (EC, Salinity, chloride, sulfate, calcium, magnesium, and sodium) (Table 2) reveals several relevant hydrochemical relationships. These are (1) the strong and positive correlations that distinguish the correlations of sodium, chloride, calcium, magnesium, and sulfate versus the salinity (>0.9), suggest that the referred elements have largely influenced the composition of groundwater resources; (2) the well-defined relationship between Na and Cl ($r = 0.96$) confirms the same origin of these elements probably related to the halite dissolution; (3) the positive correlation between Mg and SO_4 ($r = 0.94$) indicates that these ions originate from the Mg-sulfate dissolution; and (4) the positive relationship between Ca and SO_4 ($r = 0.88$) likely highlights the same origin of these ions, related to the dissolution of gypsum and/or anhydrite.

Table 2. Correlation matrix of the geochemical variables

	EC	Salinity	Cl	SO4	Na	Mg	Ca
Salinity	0.98	**1**					
Cl	0.98	0.95	**1**				
SO_4	0.86	0.92	0.79	**1**			
Na	0.97	0.95	0.96	0.84	**1**		
Mg	0.88	0.92	0.81	0.94	0.82	**1**	
Ca	0.87	0.91	0.84	0.88	0.79	0.87	**1**

EC: Electrical conductivity.

Downloaded by [Amor Ben Moussa] at 02:26 04 January 2012

Downloaded by [Amor Ben Moussa] at 02:26 04 January 2012

Principal Component Analysis

The Principal component analysis (PCA) is the most common multivariate statistical method used to exhibit complex associations among several variables and individuals (Dalton & Upchurch, 1978; Fovell & Fovell, 1993; Guler et al., 2002). It permits to graphically classify the appearance of variables and samples (Cattel, 1965). This approach has allowed reducing the great number of variables to few factors basing on the loading or weight of each factor. The PCA approach started by preserving only the first two factors (F_1 and F_2) that have the most important loading and excluding the less important ones (Davis, 1986; Kumar et al., 2006). The preserved two factors represent 75.6% of total samples variance (60.25% for F_1 and 15.38% for F_2). From the position of variables on the two first main axes (Figure 4), the F_1 factor takes high positive loadings (over 0.75) for all ions, EC, and salinity, except for NO_3 and pH that show a negative loading. This major factor reveals the implication of natural mineralization processes such as the dissolution of evaporates (NaCl and $CaSO_4$. $2H_2O$). The F_2 factor takes high positive loadings for NO_3, moderate to low positive loading for Ca and SO_4 and negative loading for pH, Na. The ions behaviors expressed by this factor are interpreted as a result of anthropogenic processes such as potential contamination deriving from the application of fertilizers and the cation exchange between Na and Ca. However, the negative loading for pH that corresponds to high positive loading for the NO_3 may provide insight into the significance of the denitrification process in relation to the forest vegetation relatively abundant in these regions.

Based on the position of samples in the first factorial plan (F_1, F_2), three groundwater groups have been distinguished (Figure 5). The first group plots on the positive side of the F_1 and includes groundwater samples situated mainly in the southern part of the basin, precisely in the vicinity of the discharge areas. This may reflect the influence of natural mineralization processes which are governed by the interactions between the groundwater and the geological formations in downgradient wells. As

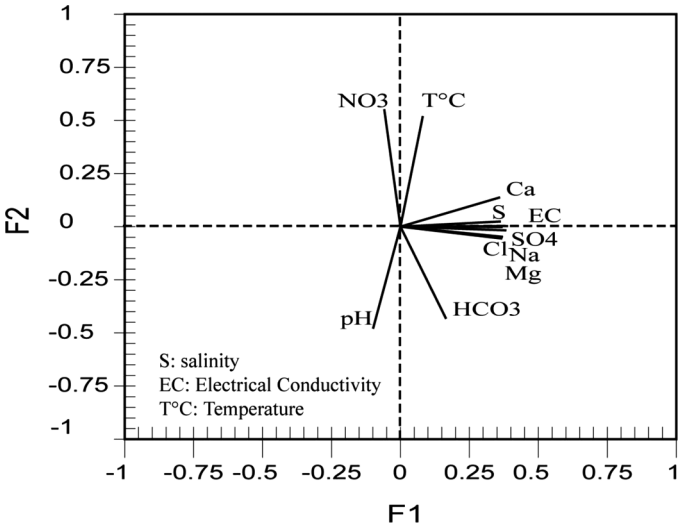

Figure 4. Variable space deduced from the geochemical PCA.

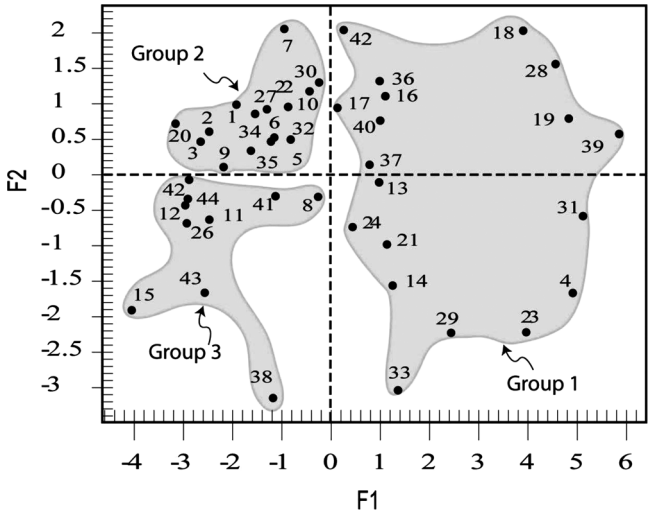

Figure 5. Cluster analysis main sample groups according to their scores for F1 and F2.

the infiltration of fresh rainwater occurs mainly in the foot of bordering highlands and in the vicinity of Wadis courses, landscape management strategies should focus on the uplands areas. Simply exploration should shift toward the high quality and renewable groundwater resources in the upper zone of the Nabeul-Hammamet basin. Moreover, steps should be taken to minimize use of saline alluvial groundwater for irrigation in areas where evaporite dissolution signatures are identified. The second group, which includes samples located mainly in the agricultural areas, in the western and east-central part of the basin, falls on the positive side of the F_2 factor and in the negative side of F_1. It is strongly associated with nitrate and could have an anthropogenic source related to the return flow of irrigation water. Therefore, several suggestions are advised. These are: (1) using the aquifer to improve the quality and security of drinking water and agricultural water supplies; (2) after considering the environmental damages caused by anthropogenic pollutants related to the application of fertilizers, it is necessary to find out whether artificial recharge will be profitable to attenuate artificial pollutants; and (3) determine the optimal amount of fertilizer application in the agricultural activity. Furthermore, this group is linked to calcium and is negatively correlated with sodium. This is typically attributed to the exchange of Na for Ca on exchange sites of clays. The third group plots in both negative sides of F_1 and F_2 and includes samples collected from wells located mainly in the recharge area and near the Wadis' courses. It is strongly associated with pH and negatively correlated with NO_3. This may reflect the significance of denitrification phenomenon that contributes to the conversion of NO_3 to N_2 by bacterial actions

Correlations of Major Ions

Relationships between major ions clearly corroborate with the results of the correlation matrix and PCA about the main mineralization processes. Dissolution of halite is confirmed, at first through the strong correlation between Na and Cl and,

Downloaded by [Amor Ben Moussa] at 02:26 04 January 2012

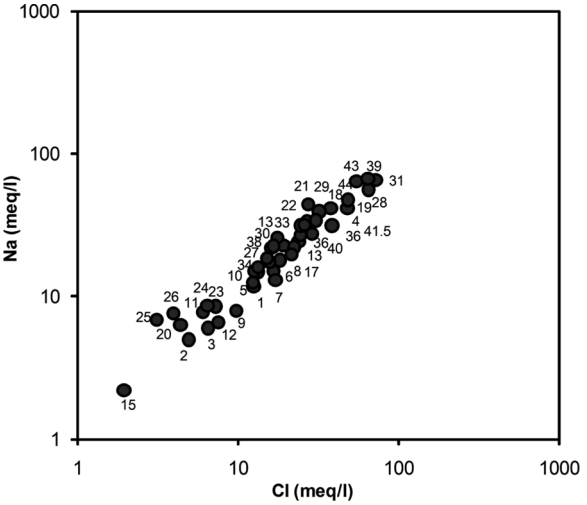

Figure 6. Plots of Na vs Cl.

secondly, by the negative saturation indices which indicate an undersaturation state with respect to the halite (Figure 6). Likewise, the positive correlation between Ca and SO_4 may indicate their same origin in relation to the dissolution of sulfate minerals. This is highlighted by the undersaturation of the groundwater with respect to gypsum and anhydrite (Kamel et al., 2005) (Figure 7).

Cation-exchange between groundwater and its host environment is highlighted, first, through the excess of sodium which is compensated by the relative deficiency of calcium and, secondly, by the calculated Base Exchange Indices, in particular the

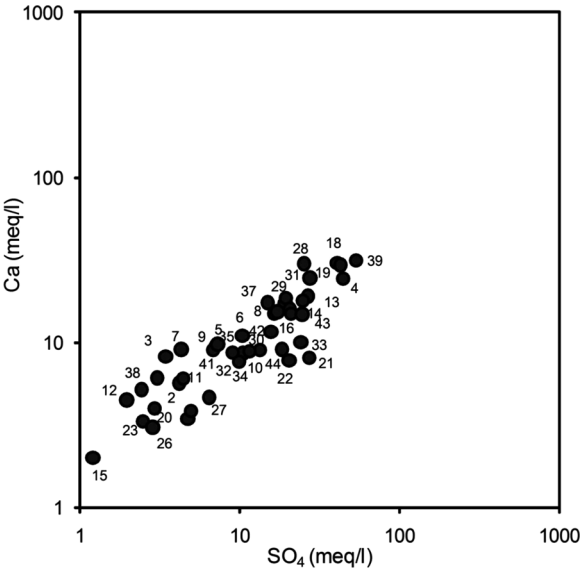

Figure 7. Plots of Ca vs SO_4.

Downloaded by [Amor Ben Moussa] at 02:26 04 January 2012

Chloro Alkaline Indices (CAI 1, 2) (Schoeller, 1965; Garcia et al., 2001). These aforementioned indices are calculated using the equations:

$$CA\,1 = Cl - \frac{Na + K}{Cl}$$

$$CAl\ \ 2 = Cl - \frac{Na + K}{SO} + HCO_3 + CO_3 + NO_3$$

If there is an exchange of Na and K from water with Mg and Ca of the rock, the exchange is known as direct and both the indices are positive. These later are negative and then the exchange is indirect when there is an exchange of Mg and Ca of the waters with Na and K of the rocks. The studied groundwater samples showed positive indices, illustrating that they had direct Base Exchange reaction (Figure 8).

On the other hand, the nitrate contents in the Nabeul-Hammamet groundwater fluctuate between 8 and 425 mg/l. Thirty three samples show high nitrate contents exceeding 50 mg/l (the World Health Organization's (WHO's) recommended maximum for drinking-water) (WHO, 2006). These high concentrations of nitrate are most likely related to the extensive agricultural activities. In the agricultural areas, young, labile Organic Matter (OM), commercial complex nitrogen fertilizers, ammonium nitrate, and other liquid fertilizer are used in large-scale amounts during the autumn and spring seasons. This fertilization is done with an amount ranging from 350 to 400 kg/ha and from 100 to 150 kg/ha for the irrigated and non-irrigated soils, respectively. In addition to the fertilizer application, the long-term flood irrigation practices highlight the significant contribution of the return flow of irrigation waters to the degradation of groundwater quality (Singh et al., 1995; Oenema et al., 1998; Hadas et al., 1999). To accurately recognize the effect of the over-fertilization practices on groundwater quality, the evolutions of NO_3, Ca, Mg, and SO_4 were established. In the agricultural area, the NO_3 and Ca ions showed comparable evolution, suggesting that the concentration of these elements are probably influenced by the large application Ca $(NO_3)_2$-fertilizers (Stigter et al., 2006) (Figure 9). Moreover, samples collected from agricultural areas display similar chemical tendency between

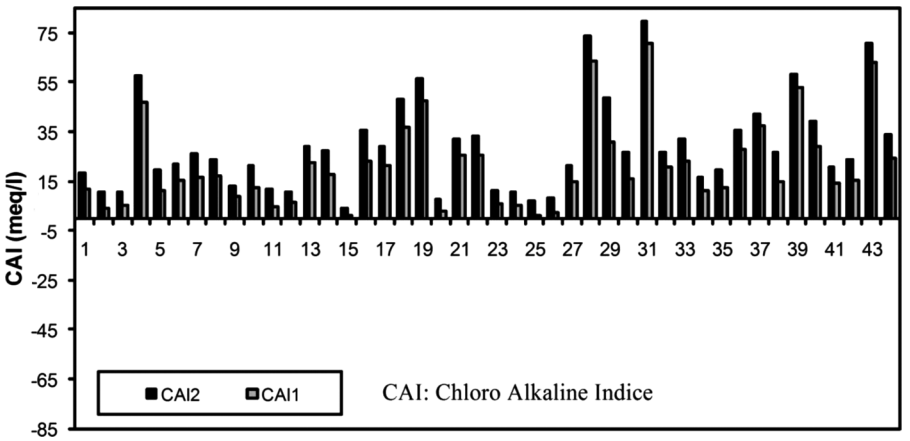

Figure 8. CAI1 and CAI2 of the unconfined aquifer groundwaters.

Downloaded by [Amor Ben Moussa] at 02:26 04 January 2012

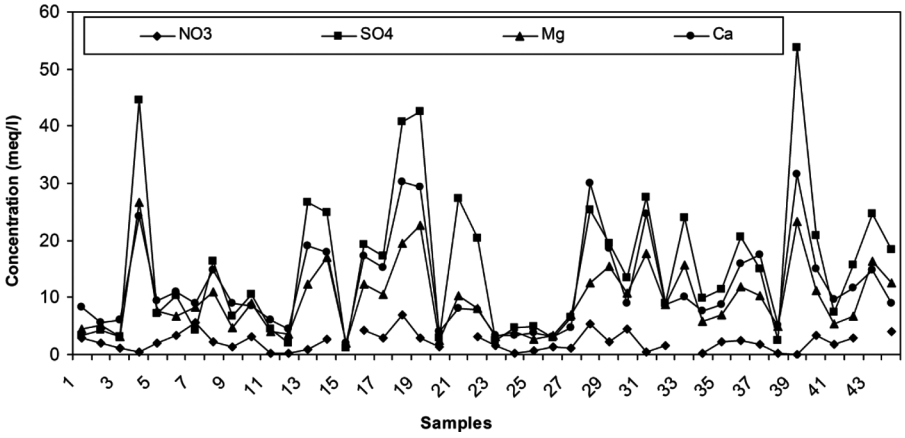

Figure 9. Relationship showing the evolution of NO_3, Ca, Mg and SO_4.

nitrate and SO_4, which provide insight into the use of N and S in the form of $(NH_4)_2SO_4$ (Gi-Tak et al., 2004; Bohike et al., 2007) (Figure 9). Therefore, there is a fundamental need for rapid assessment of the aquifer contamination trough the fertilizer application.

On the other hand, samples that show relatively low nitrate levels are found throughout the area north of the basin. In these regions, clayey deposits contribute to the diminution of rainwater infiltration and generate anaerobic conditions encouraging denitrification process during which NO_3 converts to N_2 by bacterial activities. The bacteria utilize NO_3 as an oxidant in the anaerobic water conditions. Thus, over-fertilization can engender an increasing rate of return nitrogen to the atmosphere through biological denitrification (Oonk & Kroeze, 1999).

Conclusion

The present study indicates that coupling multivariate statistical techniques with hydrogeochemical analysis is an efficient way that permits discrimination between the different processes controlling the groundwater salinization in the Nabeul-Hammamet coastal plain, north-eastern Tunisia. The studied groundwater, which was divided into Ca-SO_4-Cl and Na–Cl water types, acquires its mineralization principally through natural mineralization mechanisms such as the dissolution of evaporate minerals and ion exchange. However, anthropogenic processes in relation to agricultural activities also play an important role in the salinization of groundwater. Most groundwater samples are characterized by high nitrate content in relation to the long-term flood irrigation practices and the excessive use of fertilizers. Thus, irrigation is coming under growing stress to use water efficiently. Indeed, excess irrigation in conjunction with over-fertilization have engendered deleterious effects on the environment through water contamination and increased soil salinity. As a result, understanding environmental consequences of agricultural practices is essential to reduce unintended, deleterious problems. The improvement of our natural resources can be accomplished through assessing the success of management practices and by adjusting conservation policies as required to ensure long-term protection.

Downloaded by [Amor Ben Moussa] at 02:26 04 January 2012

References

Adams, S., G. Tredoux, C. Harris, R. Titus, and K. Pietersen. 2001. Hydrochemical characteristics of aquifers near Sutherland in the Western Karoo, South Africa. *Journal of Hydrology* 241: 91–103.

Ball, J. W., and D. K. Nordstrom. 1991. *WATEQ4F—User's manual with revised thermodynamic database and test cases for calculating speciation of major, trace and redox elements in natural waters*. United States Geological Survey, Open-File Report, 90–129.

Ben Salem, H. 1995. Évolution de la péninsule du cap Bon (Tunisie orientale) au cours du Néogène [Evolution of the Cap Bon peninsula during Neogene]. *Notes Service Géologique, Tunisie* [Notes Geological Survey, Tunisia] 61: 73–84.

Blondel, J. A. T. 1991. Les séries à tendance transgressive marine du Miocène inférieur à moyen de la Tunisie centrale [Trangressive series of the Lower and middle Miocene in central Tunisia]. PhD Thesis, University of Genova, Italy.

Bohike, J. K., R. L. Smith, and J. E. Hannon. 2007. Isotopic analysis of N and O in nitrite and 383 nitrate by sequential selective bacterial reduction to N_2O. *Analytical Chemistry* 79(384): 5888–5895.

Burollet, P. F. 1956. Contribution à l'étude stratigraphique de la Tunisie centrale [Contribution in the study stratigraphy of central Tunisia]. *Annale des mines et de la géologie* [Annals of Mines and Geology], 345.

Cattel, R. B. 1965. Factor analysis: Introduction to essentials. *Biometrics* 2: 405–435.

Chadha, D. K. 1999. A new diagram for geochemical classification of natural waters and interpretation of chemical data. *Hydrogeology Journal* 7: 431–439.

Colleuil, B. 1976. Etude stratigraphique et néotectonique des formations néogènes et quaternaires de la région de Southern Cap Bon [Stratigraphic and neotectonic study of neogene and quarternay formations of the southern Cap Bon] (Cap Bon) D.E.S., Nice University.

Dalton, M. G., and S. B. Upchurch. 1978. Interpretation of hydrochemical facies by factor analysis. *Groundwater* 16: 228–233.

Davis, J. C. 1986. *Statistics and data analysis in geology*. Wiley, New York.

Fovell, R., and M. Y. Fovell. 1993. Climate zones of the conterminous United States defined using cluster analysis. *Journal of Climate* 6: 2103–2135.

Garcia, M. G., M. Del Hidalgo, and M. A. Blesa. 2001. Geochemistry of groundwater in the alluvial plain of Tucuman province. Argentina. *Hydrogeology Journal* 9: 597–610.

Gi-Tak, C., K. Kangjoo, T. Seong, H. Kyoung, O. Soon, Y. Byoung, S. Hyoung, and W. Chul. 2004. Hydrogeochemistry of alluvial groundwaters in an agricultural area: An implication for groundwater contamination susceptibility. *Chemosphere* 55: 369–378.

Guler, C., G. D. Thyne, J. E. McCray, and A. K. Turner. 2002. Evaluation of graphical and multivariate statistical method for classification of water chemistry data. *Hydrogeology Journal* 10(C4): 455–474.

Hadas, A., B. Sagiv, and N. Haruvy. 1999. Agricultural practices, soil fertility management modes and resultant nitrogen leaching rates under semi-arid conditions. *Agricultural Water Management* 42: 81–95.

Helena, B., B. Pardo, M. Vega, E. Barrado, J. M. Fernandez, and L. Fernandez. 2000. Temporal evolution of groundwater composition in an alluvial aquifer (Pisuerga River, Spain) by principal component analysis. *Water Research* 34: 807–816.

Kamel, S., L. Dassi, K. Zouari, and B. Abidi. 2005. Geochimical and isotopic investigation of the aquifer system in the Djerid-Nefzaoua basin, southern Tunisia. *Environmental Geology* 49: 159–170.

Kumar, M., A. L. Ramanathan, M. S. Rao, and B. Kumar. 2006. Identification and evaluation of hydrogeochemical processes in the groundwater environment of Delhi, India. *Environmental Geology* 50: 1025–1039.

Downloaded by [Amor Ben Moussa] at 02:26 04 January 2012

Mzali, H., H. Gabtni, H. Zouari, M. Hadj Sassi, and J. Gharsalli. 2007. Evidence of N120 shear corridors and associated tectonic structures in north-eastern Tunisia based on geological and geophysical data. *Comptes Rendus Geoscience* 339: 358–365.

Mzali, H., and H. Zouari. 2006. Caractérisation géométrique et cinématique des structures liées aux phases compressives de l'Éocène au Quaternaire inférieur en Tunisie: Exemple de la Tunisie nord-orientale [Characterization of geometric and kinematic structures related to the Eocene and the Late Quarternay compressive phases in Tunisia: Example of North-Oriental Tunisia]. *Comptes Rendus Geoscience* 338: 742–749.

Oenema, O., P. C. M. Boers, M. M. van Eerdt, B. Fraters, H. G. van der Meer, C. W. J. Roest, J. J. Schroder, and W. J. Willems. 1998. Leaching of nitrate from agriculture to groundwater: the effect of policies and measures in the Netherlands. *Environmental Pollution* 102: 471–478.

Oonk, H., and C. Kroeze. 1999. Nitrous oxide emissions and control, pp. 1055–1069, in R. A. Meyers, ed., *Encyclopedia of environmental pollution and cleanup*. Wiley, New York.

Rightmire, C. T. 1978. Seasonal variation in pCO_2 and ^{13}C content of soil atmosphere. *Water Resources Research* 14: 691.

Schoeller, H. 1939. Le Quaternaire du Golfe ancien de Grombalia, Tunisie. *Actes Société Linnéenne de Bordeaux* 91: 14–30.

Schoeller, H. 1965. Hydrodynamique lans le karst. *Actes du Colloque de Dubrovnik*, IAHS/UNESCO, 3–20.

Singh, B., Y. Singh, and G. S. Sekhon. 1995. Fertilizer-N use efficiency and nitrate pollution of groundwater in developing countries. *Journal of Contaminant Hydrology* 20: 167–184.

Stigter, T. Y., A. M. Carvalho, L. Ribeiro, and E. Reis. 2006. An Impact of the shift from groundwater to surface water irrigation on aquifer dynamics and hydrochemistry in a semi-arid region in the south of Portugal. *Agricultural Water Management* 85: 121–132.

World Health Organization (WHO). 2006. *Guidelines for drinking water quality. 3rd ed.* incorporating first addendum. http://www.who.int/water_sanitation_health/dwq/gdwq3rev/en/index.html (Accessed 2009).

Downloaded by [Amor Ben Moussa] at 02:26 04 January 2012